Supporting Information

Aqueous Solution Processable Metal Oxides For High-Performance Organic and Perovskite Solar Cells

Yan-Hui Lou,[a,b] and Zhao-Kui Wang[a,*]

[a]Jiangsu Key Laboratory for Carbon-Based Functional Materials & Devices, Institute of Functional Nano & Soft Materials (FUNSOM), Soochow University, Suzhou, Jiangsu 215123, China

[b]College of Physics, Optoelectronics and Energy, Soochow University, Suzhou 215123, China

[*]Address correspondence to zkwang@suda.edu.cn (Z.K. Wang)

Table of Contents

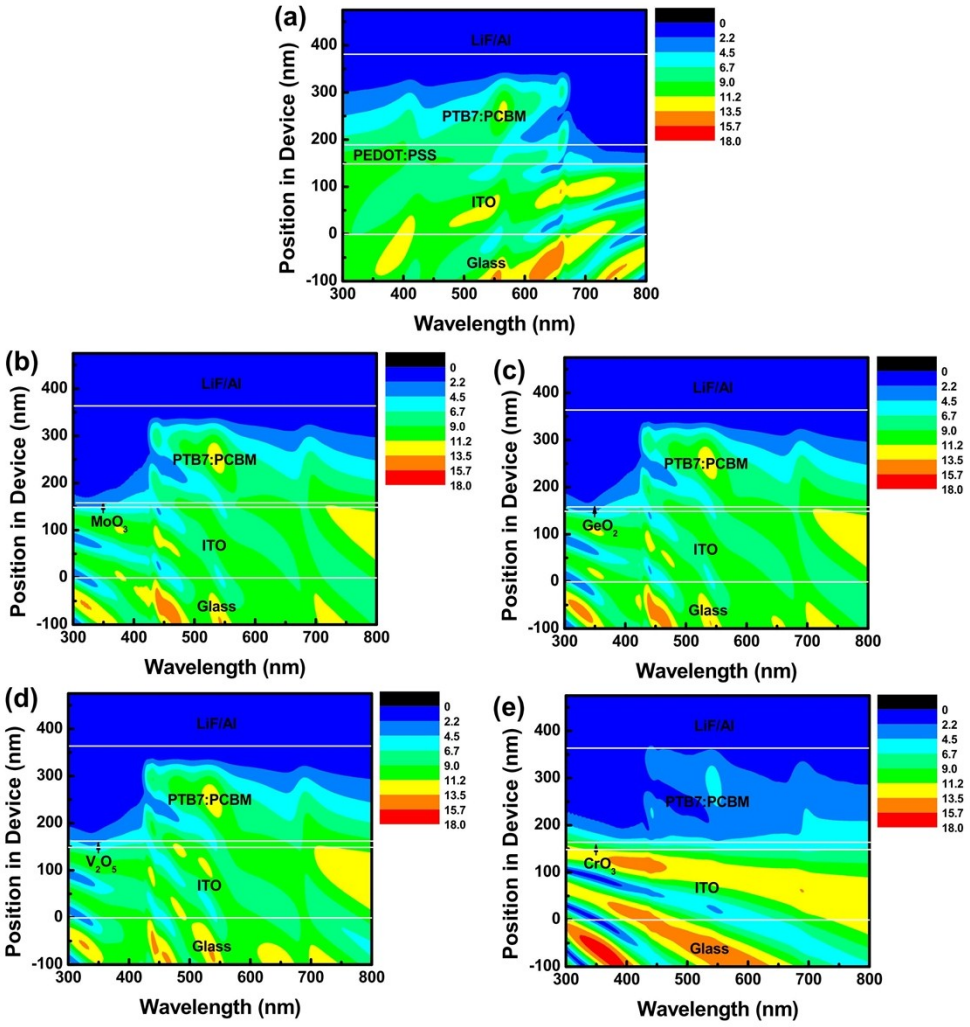

Figure S1. Optical field ($|E|^2$) distributions in PTB7:$PC_{71}BM$ based bulk heterojuncion solar cells incorporting with differnt hole transporting layers of (a) PEDOT:PSS, (b) *s*MoO_3, (c) *s*GeO_2, (d) *s*V_2O_5 and (e) *s*CrO_3. Calculation were carried out under the consideration of the whole visible light range (300~800 nm).

Impedence Spectra Evaluations of the Anode Interfaces

Device structure:

ITO/TMOs (*s*MoO_3, *s*GeO_2, *s*V_2O_5, or *s*CrO_3)/PTB7:$PC_{71}BM$/MoO_3/Al

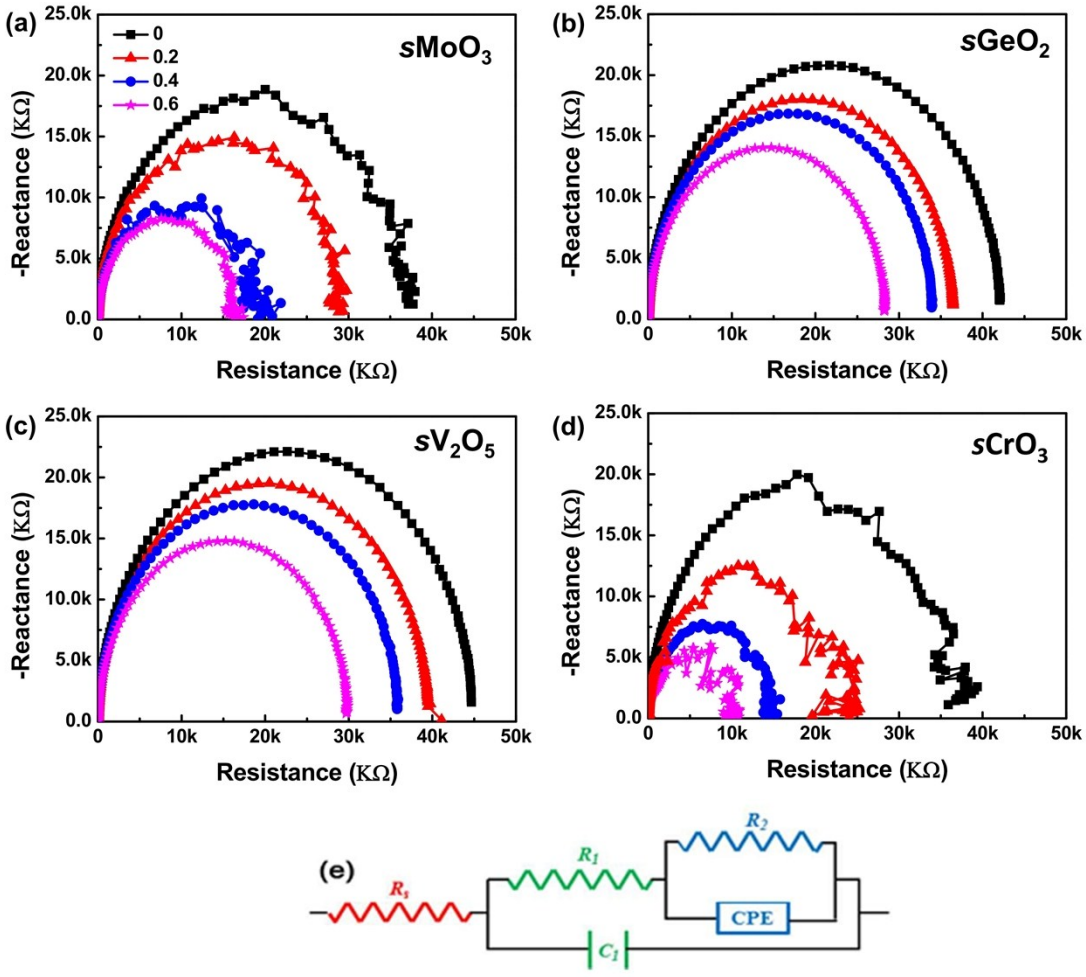

Figure S2. Impedance response in PTB7:$PC_{71}BM$ based hole-dominant devices incorporating with different aqueous solution processed hole transporting layers (a) *s*MoO_3, (b) *s*GeO_2, (c) *s*V_2O_5 and (d) *s*CrO_3. (e) Equivalent circuit used to fi t the data in (a)- (d). Rs represents the resistive losses in the ITO and sTMOs.

Impedence Spectra Evaluations of the Anode Interfaces

Device structure:

ITO/TMOs (*s*MoO_3, *s*GeO_2, *s*V_2O_5, or *s*CrO_3)/PTB7:$PC_{71}BM$/MoO_3/Al

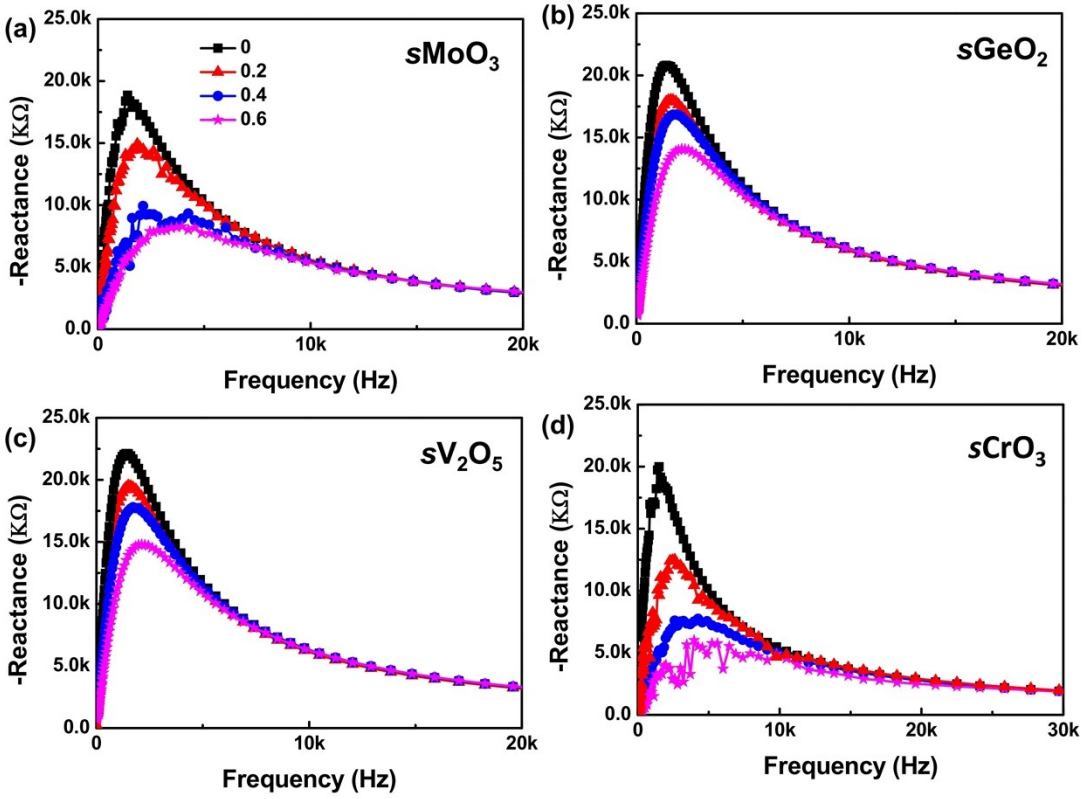

Figure S3. Reactance-frequency relations in PTB7:$PC_{71}BM$ based hole-dominant devices incorporating with different aqueous solution processed hole transporting layers (a) *s*MoO_3, (b) *s*GeO_2, (c) *s*V_2O_5 and (d) *s*CrO_3.

Device Optimization of *s*TMOs Based Perovskite Solar Cells

Device structure:

ITO/ TMOs (*s*MoO_3, *s*GeO_2, *s*V_2O_5, or *s*CrO_3)/$CH_3NH_3PbI_{3-x}Cl_x$/$PC_{61}BM$/Ag

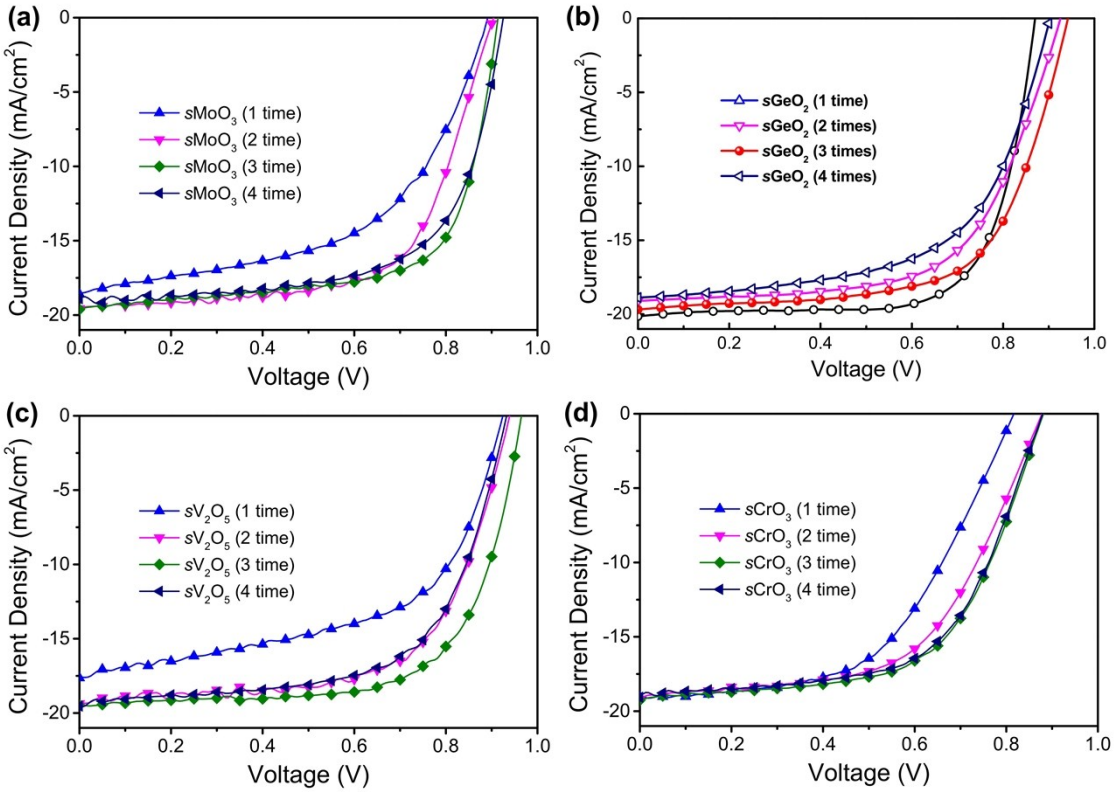

Figure S4. *J-V* curves of perovskite solar cells using different *s*TMO as the HTLs under AM 1.5G illumination of 100 mW cm^2.

Table S1. Cell parameters of perovskite solar cells using different *s*TMO as HTLs

HTL	J_{SC} (mA/cm^2)	V_{OC} (V)	FF	PCE (%)
sMoO_3 (1 time)	18.58	0.89	0.53	8.79
sMoO_3 (2 time)	19.56	0.90	0.64	11.36
sMoO_3 (3 time)	19.61	0.91	0.68	12.23
sMoO_3 (4 time)	18.90	0.92	0.66	11.47
sGeO_2 (1 time)	18.63	0.88	0.55	8.95
sGeO_2 (2 time)	19.27	0.92	0.62	11.02
sGeO_2 (3 time)	19.62	0.94	0.66	12.12
sGeO_2 (4 time)	18.95	0.90	0.60	10.37
sV_2O_5 (1 time)	17.63	0.92	0.56	9.10
sV_2O_5 (2 time)	19.36	0.94	0.65	11.71
sV_2O_5 (3 time)	19.46	0.96	0.68	12.75
sV_2O_5 (4 time)	19.53	0.93	0.63	11.46
sCrO_3 (1 time)	19.04	0.81	0.54	8.33
sCrO_3 (2 time)	19.17	0.87	0.57	9.48
sCrO_3 (3 time)	19.26	0.88	0.60	10.15
sCrO_3 (4 time)	19.06	0.88	0.60	9.98

Device Optimization of PEDOT:PSS-TMOs Based Perovskite Solar Cells

Device structure:

ITO/ PEDOT:PSS-TMOs (*s*MoO_3, *s*GeO_2, *s*V_2O_5, or *s*CrO_3)/$CH_3NH_3PbI_{3-x}Cl_x$/$PC_{61}BM$/Ag

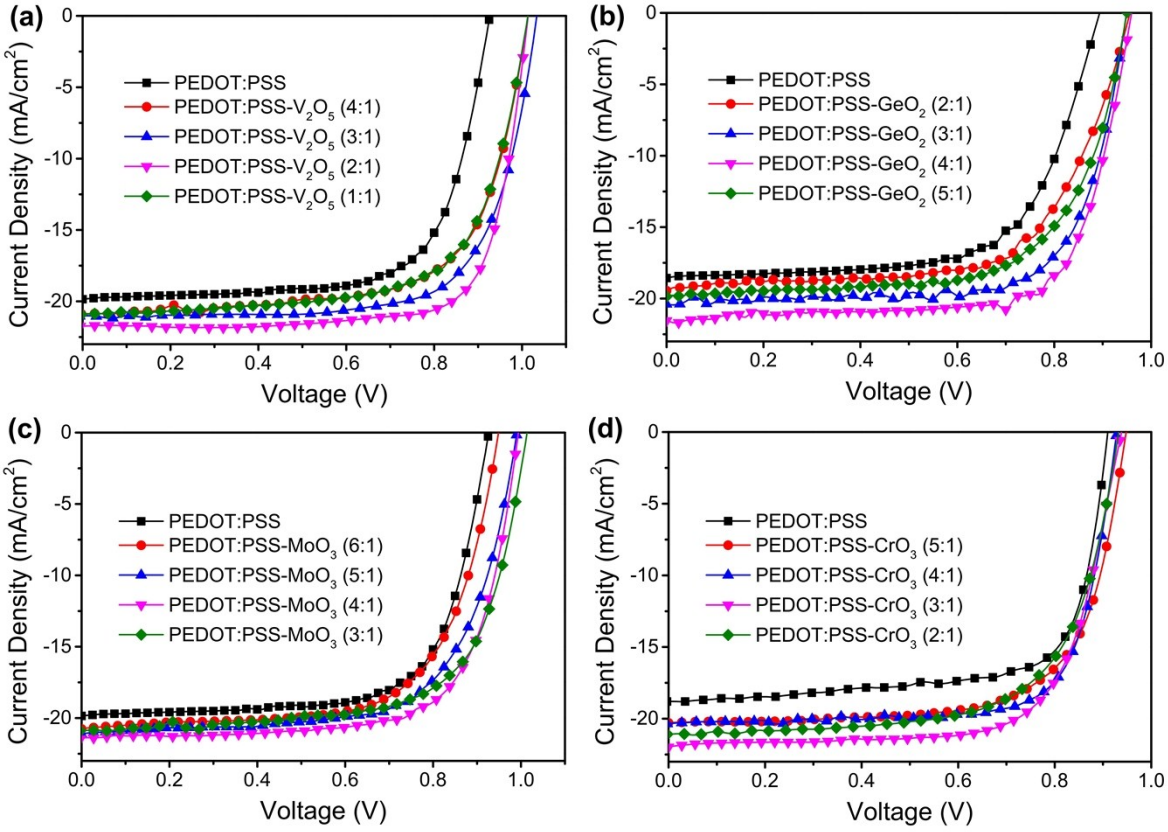

Figure S5. *J-V* curves of perovskite solar cells using different PEDOT:PSS-TMO as the HTLs under AM 1.5G illumination of 100 mW cm^2.

Table S2. Cell parameters of perovskite solar cells using PEDOT:PSS-TMOs as HTLs

HTL	J_{SC} (mA/cm^2)	V_{OC} (V)	FF	PCE (%)
PEDOT:PSS	20.64	0.86	0.68	12.08
PEDOT:PSS-MoO_3 (6:1)	21.25	0.94	0.67	13.05
PEDOT:PSS-MoO_3 (5:1)	21.11	0.99	0.67	14.03
PEDOT:PSS-MoO_3 (4:1)	21.38	0.99	0.72	15.10
PEDOT:PSS-MoO_3 (3:1)	20.86	1.01	0.68	14.32
PEDOT:PSS	20.54	0.93	0.74	14.13
PEDOT:PSS-V_2O_5 (4:1)	20.86	1.01	0.68	14.32
PEDOT:PSS-V_2O_5 (3:1)	21.02	1.02	0.72	15.56
PEDOT:PSS-V_2O_5 (2:1)	22.38	1.02	0.79	18.03
PEDOT:PSS-V_2O_5 (1:1)	20.90	1.01	0.67	14.48
PEDOT:PSS	18.57	0.89	0.67	10.97
PEDOT:PSS-GeO_2 (5:1)	19.84	0.94	0.67	12.50
PEDOT:PSS-GeO_2 (4:1)	21.55	0.96	0.74	15.15
PEDOT:PSS-GeO_2 (3:1)	20.39	0.95	0.72	13.86
PEDOT:PSS-GeO_2 (2:1)	19.44	0.96	0.65	12.10
PEDOT:PSS	18.79	0.91	72	12.37
PEDOT:PSS-CrO_3 (5:1)	20.29	0.94	70	13.33
PEDOT:PSS-CrO_3 (4:1)	20.32	0.93	75	14.09
PEDOT:PSS-CrO_3 (3:1)	21.97	0.94	71	14.50
PEDOT:PSS-CrO_3 (2:1)	21.07	0.93	67	13.13

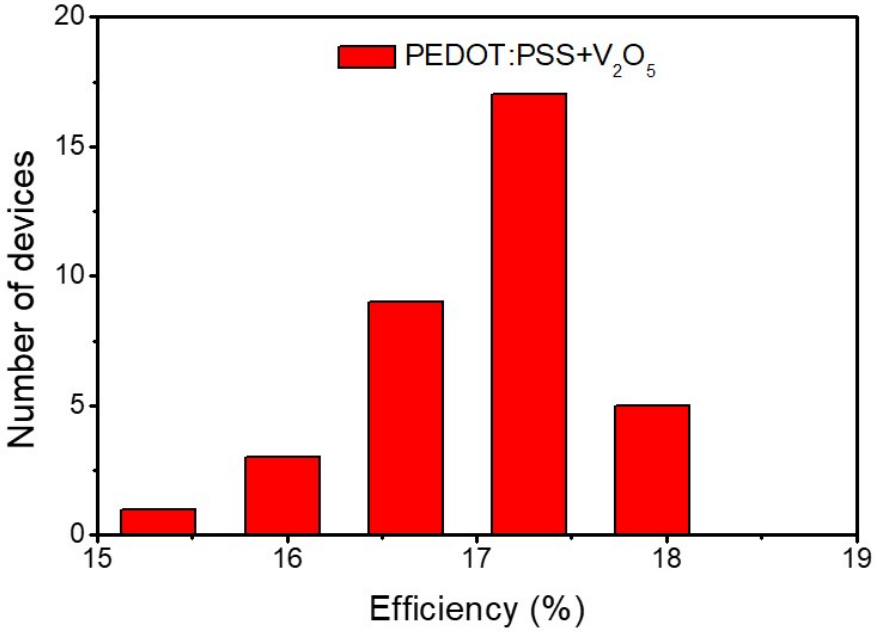

Figure S6. A histogram of PCEs measured from 35 PEDOT:PSS-V_2O_5 HTL based perovskite solar cells.

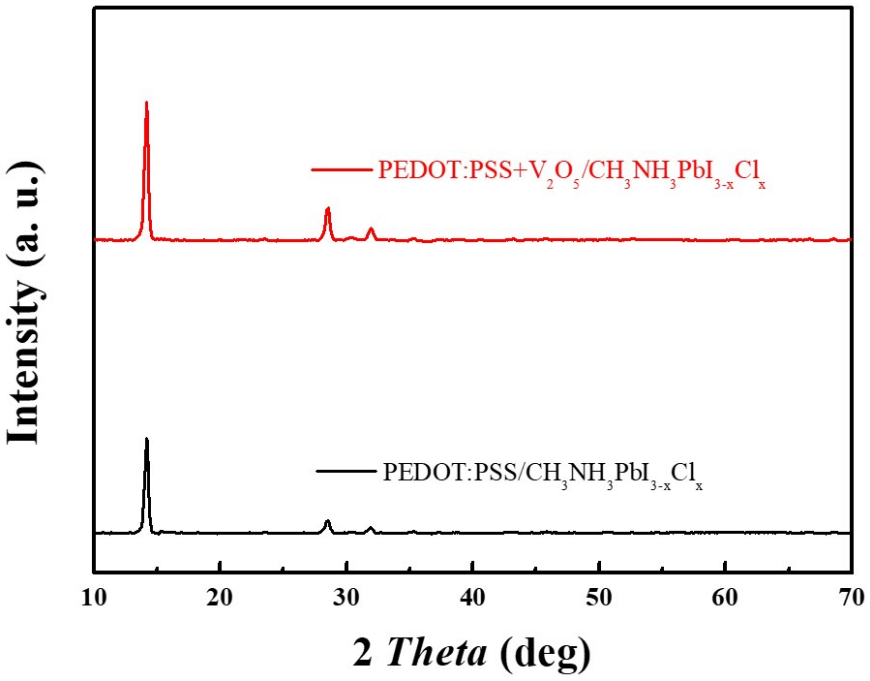

Figure S7. XRD patters of polycrystalline $CH_3NH_3PbI_{3-x}Cl_x$ films deposited on PEDOT:PSS and PEDOT:PSS+V_2O_5 underlayers.

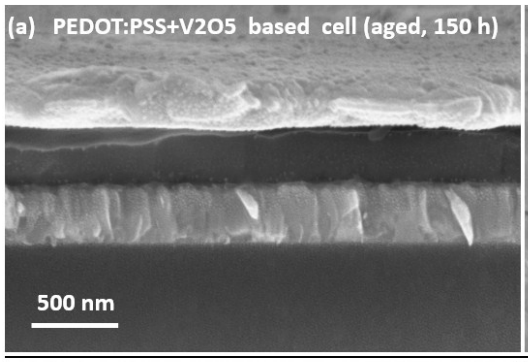

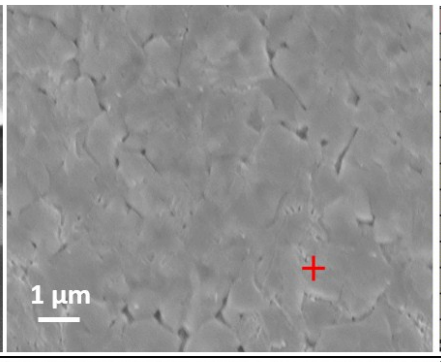

Element	Wt%	At%
CK	21.33	24.74
NK	74.74	74.42
OK	00.10	00.00
CuL	00.95	00.21
NaK	00.37	00.22
SiK	00.12	00.06
PbM	00.67	00.05
ClK	00.18	00.07
InL	00.53	00.06
CaK	00.27	00.09
IL	00.75	00.08
Matrix	Correction	ZAF

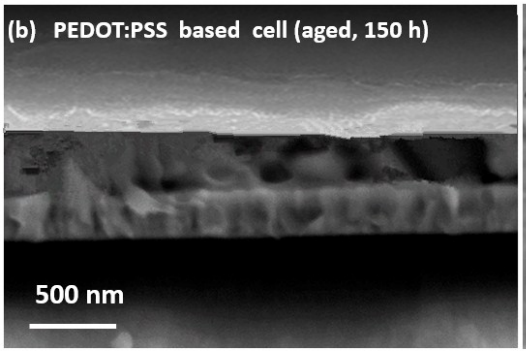

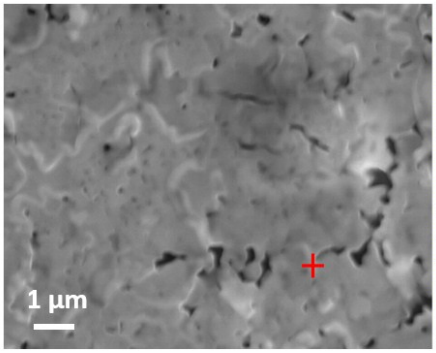

Element	Wt%	At%
CK	81.48	94.46
NK	00.00	00.00
OK	09.40	03.60
CuL	01.68	00.35
NaK	00.92	00.52
SiK	00.33	00.15
PbM	01.71	00.11
ClK	00.80	00.29
InL	01.81	00.21
CaK	00.49	00.16
IL	01.38	00.14
Matrix	Correction	ZAF

Figure S8. Cross-sectional SEM and EDX analysis of (a) PEDOT:PSS+V_2O_5 based and (b) PEDOT:PSS based perovskite solar cells (aged, 150h).